Available online at www.sciencedirect.com
ScienceDirect
Journal of Power Sources 160 (2006) 897–902
JOURNAL OF POWER SOURCES
www.elsevier.com/locate/jpowsour

Ceria coated Ni as anodes for direct utilization of methane in low-temperature solid oxide fuel cells

Wei Zhu, Changrong Xia *, Jue Fan, Ranran Peng, Guangyao Meng

Laboratory for Biomass Clean Energy, Department of Materials Science and Engineering, University of Science and Technology of China, Hefei, 230026 Anhui, China

Received 14 December 2005; received in revised form 5 February 2006; accepted 6 February 2006
Available online 23 March 2006

Abstract

A new type of anode, a Ni framework coated with Sm-doped ceria (SDC), was developed for direct utilization of methane fuel in low-temperature solid oxide fuel cells (SOFCs) with thin-film SDC electrolytes. The coated SDC was prepared with an ion impregnating method and the electrolyte films were fabricated with a co-pressing and co-firing technique. The impregnating process produced an ideal anode microstructure where nickel particles were effectively connected and uniformly covered with nanosized SDC. This anode microstructure was believed to enlarge the triple-phase boundaries and therefore enhance the anode performance. The cell performance was much higher than that of a conventional fuel cell with a Ni-SDC composite anode. In addition, the performance increased with impregnated SDC loading up to a maximum at 20 mg cm^{-2}, indicating that the coated SDC is the contributing factor for the enhanced fuel cell performance. Power density as high as 571 and 353 mW cm^{-2} were obtained at 600 °C when humidified hydrogen and methane were used as fuels, respectively. The stability of the cell also increased with the SDC loading. No significant degradation was observed for anodes coated with 20 and 25 mg cm^{-2} SDC. This verifies that the coated SDC electrodes are very effective in suppressing catalytic carbon formation by blocking methane from approaching the Ni, which is catalytically active towards methane pyrolysis. The high performance of this anode shows high promise in the developing field of direct hydrocarbon SOFCs.

Keywords: Solid oxide fuel cells; Low-temperature SOFCs; Direct hydrocarbon fuel cells; Impregnating; Doped ceria

1. Introduction

It is desirable to develop solid oxide fuel cell (SOFC) systems in which the hydrocarbons are fed to the fuel cell directly without significant amounts of water or oxygen [1]. There are basically two strategies to achieve such SOFCs. The first involves conventional cermet anodes. Ni cermet anodes, on which the most advanced SOFCs are based, have been extensively studied for direct utilization of hydrocarbons [2]. Since nickel catalyzes the formation of carbon, which rapidly deactivates the fuel cell, the Ni-cermets can only be used under conditions in which carbon does not form. The conditions are usually restricted to thermodynamically stable composition and temperature regimes. However, the operation still requires the exercise of caution, given that carbon can form catalytically on Ni surfaces and the carbon formation is more likely to be related to kinetic rather than to thermodynamic considerations. One solution for avoiding carbon-deposition problems associated with Ni-based anodes, is to replace Ni with Cu [3,4], which is not a catalyst for carbon formation. However, Cu is not a good oxidation catalyst and has a relatively low melting temperature, which decreases the anode stability. Further, the low melting temperature of copper oxides makes the fabrication procedures typically used for Ni-cermets impossible. The second strategy is to use ceramic materials, which do not catalyze carbon formation. Among these materials, highly conductive perovskites have received much attention for direct hydrocarbon conversion in SOFCs. For example, Tao and Irvine demonstrated that a $(La_{0.75}Sr_{0.25})_{0.9}Cr_{0.5}Mn_{0.5}O_3$ based anode is effective for 3% H_2O humidified CH_4 [5]. Doped ceria is also used as a ceramic anode for direct hydrocarbon conversion. Interesting properties have been primarily demonstrated by Steele and co-workers for ceria-based anodes in direct utilization of methane [6]. Further work has shown that the performance was too low for practical considerations. The reason is most

* Corresponding author. Tel.: +86 551 3607475; fax: +86 551 3606689.
E-mail address: xiacr@ustc.edu.cn (C. Xia).

0378-7753/$ – see front matter © 2006 Elsevier B.V. All rights reserved.
doi:10.1016/j.jpowsour.2006.02.020

likely due to insufficient electronic conductivity of the doped ceria. Later work by Marina and co-workers has shown excellent performance for a Gd-doped ceria anode, which is 10–15 μm thick with an Au-GDC composite layer as the current-collector [7]. It has been argued that this anode is essentially an Au-GDC composite with Au providing the electronic conduction. Nevertheless, it does imply that doped ceria is an excellent catalyst for electrochemical oxidation of hydrocarbons.

In this work, an alternative anode is explored for direct utilization of hydrocarbons. The anode is based on an electronic conducting framework covered with doped ceria. Nickel is used as the framework to ensure electronic conduction and to make the co-firing technique applicable to SOFC fabrication. Doped ceria, which is a poor catalyst for carbon formation and a good catalyst for electrochemical oxidation, is used to coat nickel to block hydrocarbon from accessing to Ni surface. Consequently, the catalytic reaction of carbon deposition is expected to be effectively prevented while the electrochemical reaction is likely to be enhanced since a large ceria surface is exposed to the hydrocarbon fuels. Here we report such an anode system in a low-temperature SOFC using a thin-film electrolyte of Sm-doped ceria (SDC). The electrolyte was fabricated with a co-press/co-fire technique. SDC was coated with an ion impregnating method, which has been recently developed to introduce nanosized oxides into a SOFC electrode structure at relative low temperatures to increase the electrode performance [8,9].

2. Experimental

SDC ($Sm_{0.2}Ce_{0.8}O_{1.9}$) powders were prepared using a glycine–nitrate method as described elsewhere [10]. A solution containing Sm^{3+} and Ce^{4+} was prepared by dissolving $Sm(NO_3)_3$ and $Ce(NH_4)_2(NO_3)_6$ in distilled water with a molar ratio of Sm^{3+}:Ce^{4+} = 1:4. After adding glycine, the solution was heated till self-combustion occured. The resulted ash was heated at 600 °C for 2 h and 800 °C for 4 h to form SDC powders, which were used in electrolytes and electrodes. NiO and SSC ($Sm_{0.5}Sr_{0.5}CoO_3$, as cathode) powders were also prepared using the glycine–nitrate process. Bi-layer pellets consisted of porous NiO–SDC substrates and dense SDC electrolytes were fabricated using a co-press process [11,12]. The porous substrates were derived from NiO–SDC powders with 10 wt.% starch as pore former. SDC, with 10 wt.% in the oxides, was used to enhance the bonding between the substrate and electrolyte, and to increase the mechanical strength of the substrates. The bi-layer was co-fired at 1250 °C in air for 5 h to densify the SDC electrolyte. The thicknesses of the porous substrate and dense electrolyte were about 0.4 mm and 35 μm, respectively. The diameter of the fired pellet was 11.2 mm.

The porous NiO–SDC layer was then impregnated under vacuum with a $Sm(NO_3)_3$ and $Ce(NO_3)_3$ aqueous solution where the Sm–Ce ratio was 1:4. After drying, the pellet was calcined at 800 °C for 2 h to form SDC oxide. The loading of SDC was determined by weighing the samples before and after the impregnating process. The impregnation and calcination cycle was repeated to increase the SDC loading. A loading of 15 mg cm^{-2} required five cycles, while nine cycles resulted in 25 mg cm^{-2}. The impregnated SDC loading at different cycles is listed in Table 1, where the porosity and SDC volume fraction are also shown. The porosity was measured by the Archimedes method.

After impregnation, cathode slurry consisting of SSC–SDC having a weight ratio of 7:3 and a binder was applied to the electrolyte to form a single cell. The cell was then sealed in an alumina tube with a glass sealant. The glass sealing as well as the gas-tubing system were gas-tight as checked with a gas chromatograph (GC9750, Fuli). Two silver wires were attached to the anode and cathode with a silver paste (DAD-87 from the Shanghai Research Institute of Synthetic Resins). Electrochemical characterizations were performed at 600 °C under ambient pressure. Humidified (3% H_2O) hydrogen and methane were used as fuel and stationary air as oxidant. The current–voltage curves and stability were obtained using a potentiostat/galvanostat (DJS-292, SPSIC). The electrochemical impedance spectra were measured using an Electrochemical Workstation (IM6e, Zahner) under open circuit conditions in the typical frequency range from 0.1 Hz to 100 kHz. The morphologies were characterized with a scanning electron microscope (JSM-6700F, JEOL).

3. Results and discussion

3.1. Cell performance with hydrogen as fuel

Shown in Fig. 1 are the cell voltages and power densities at 600 °C as a function of current density for the cells with humidified (3% H_2O) H_2 as fuel. The performance of the different cells in terms of the open circuit voltage (V_{oc}) and maximum power density are summarized in Table 2. V_{oc}s are found to be between 0.881 and 0.902 V, which are similar to typical values achieved for SOFCs with ceria-based electrolytes[13,14]. The relative low V_{oc} is believed to be due to the mixed ionic and electronic conduction of the ceria electrolyte in the reducing environment, not caused by the leakage through either the glass sealant or the electrolyte film. The fuel cell system, including the sealing material and electrolyte film, was proved to be gas-tight by

Table 1
SDC loading and porosity (ρ) of anodes

Cell	No. of loading cycles	Impregnated SDC loading (mg cm^{-2})	Measured ρ before reduction (vol.%)	Measured ρ after reduction (vol.%)	Calculated SDC volume fraction (vol.%)
I	0	0	30.5	51.7	5.8
II	5	15 ± 0.2	20.6	47.0	9.9
III	7	20 ± 0.2	19.7	45.4	11.2
IV	9	25 ± 0.2	18.8	43.6	12.6

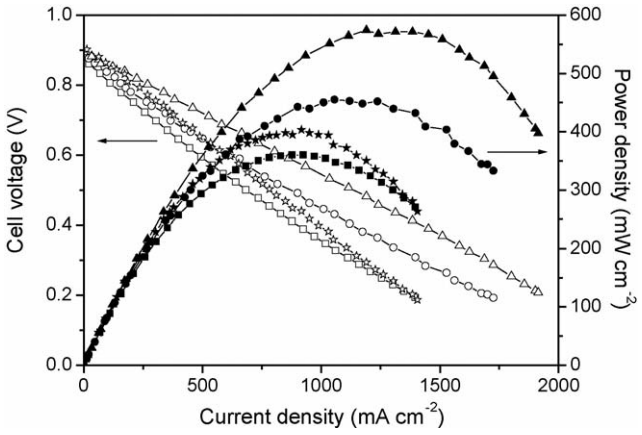

Fig. 1. Cell potentials (open symbols) and power densities (solid symbols) as a function of current density at 600 °C for cell I (square), cell II (circle), cell III (triangle) and cell IV (star) with humidified H_2 as fuel.

analyzing the outlet gas from the anode side using a gas chromatograph before and after humidified H_2 was applied to the cell. In our previous study [15], a cell based on an SDC electrolyte had achieved a maximum power density of 491 mW cm^{-2} at 600 °C when humidified hydrogen was used as the fuel. The electrical output of cell I was 131 mW cm^{-2} lower than that of the previously reported performance. Although the two cells consisted of the same cathodes and electrolytes with identical thickness, their anodes were quite different. The anode in the previous study was derived from a powder comprised of 35 wt.% SDC and 65 wt.% NiO while anode of cell I was made from 10 wt.% SDC and 90 wt.% NiO. The poor performance exhibited in cell I was possibly caused by its anode microstructure since the anode had 42.5 vol.% Ni and only 5.8 vol.% SDC, resulting in a very small triple-phase boundary (TPB) length. Further, it was observed that the maximum power density increased with increase of SDC loading in the anode. For example, maximum power densities of 455 and 571 mW cm^{-2} were achieved with cells II and III, respectively. The improvement in cell performance seems to be due to the microstructural modification of the anode by SDC impregnation. Shown in Fig. 2 are the SEM pictures for the anode surface and cross-sectional view of cell III. For this cell, 20 mg cm^{-2} SDC was impregnated in the anode. It can be seen that the anode consisted of Ni particles with an average size of about 1 μm and the Ni particles were coated with SDC particles of submicron size. The SDC particles were observed to be distributed uniformly from the anode surface to the anode–electrolyte interface. Therefore, all the impregnated

Table 2
Open circuit voltages (V_{oc}s) and maximum power densities at 600 °C for cells with humidified H_2 and CH_4 as fuel

Cell	H_2		CH_4	
	V_{oc} (V)	P_{max} (mW cm^{-2})	V_{oc} (V)	P_{max} (mW cm^{-2})
I	0.881	360	0.857	254
II	0.886	455	0.890	325
III	0.894	571	0.896	353
IV	0.902	398	0.904	260

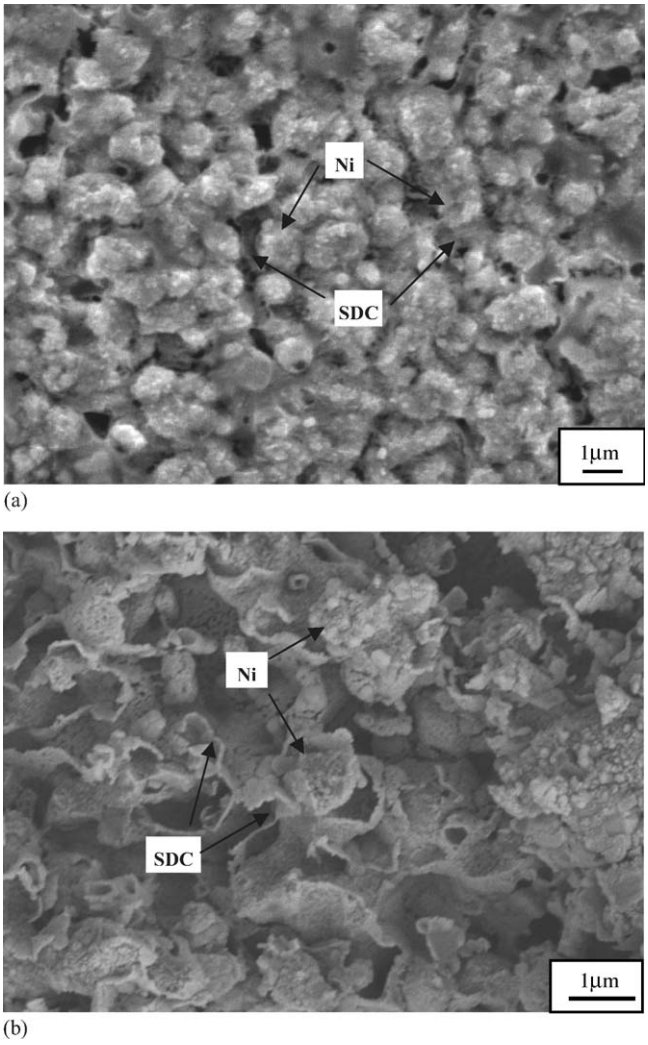

Fig. 2. SEM micrographs of (a) surface and (b) cross-section of the anode for cell III after testing.

SDC particles were connected along the surface of the Ni particles, forming a pathway for oxygen ion conduction. Eventually, the TPB was extended beyond the anode–electrolyte interface where the electrochemical oxidation possibly took place. Considering the size effect of the small SDC particles which are most likely tens of nanometers, the TPB is further enlarged, resulting in an even higher activity for the oxidation reaction. The anodic interfacial resistance, R_a, was characterized using the electrochemical impedance spectrum technique. Shown in Fig. 3 are the impedance spectra of cells I and III measured under open circuit conditions using a two-electrode configuration in humidified hydrogen. The ohmic resistances, R_r, measured from the high-frequency intercepts with the real axis are primarily due to contributions from the electrolyte and the lead wires. The interfacial resistance of the cell, R_i, determined from the difference between the high and low frequency intercepts with the real axis, is a combination of the anodic and cathodic interfacial resistances. Because of the complexity of the impedance spectra obtained with an anode-supported cell using a two-electrode configuration, it is difficult to separate the performance of one electrode from the other [16]. However, R_a can be estimated by subtract-

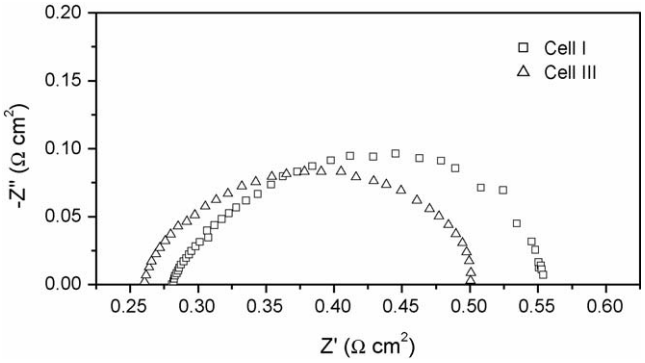

Fig. 3. Impedance spectra measured at open circuit condition for cells I and III with humidified hydrogen as fuel.

ing a typical SSC–SDC/SDC interfacial resistance, which is 0.18 Ω cm^2 at 600 °C [10]. The anode area-specific resistance (ASR), R_a, decreased from 0.092 Ω cm^2 for cell I to 0.059 Ω cm^2 for cell III. However, it increased to 0.093 Ω cm^2 for cell IV. It is obvious that the enhancement of cell performance was mainly due to the decrease in anode ASR as an effect of impregnating treatment. However, too much SDC impregnation in the anode caused an increase in the ASR and consequently resulted in poor cell performance. This implies that thicker SDC coatings on the nickel particles in the anode may actually block the gas diffusion to the TPB region and hence reduce cell performance.

3.2. Cell performance with CH_4 as the fuel

As shown in Table 2, the V_{oc} for cell I operating with methane was 0.857 V, which is much lower than 0.943 V, the potential predicted from equilibrium constant for full electrochemical oxidation reactions:

$$CH_4 + 4O^{2-} = CO_2 + 2H_2O + 8e \quad (1)$$

It is obvious that the full oxidation equilibrium was not achieved at the anode of cell I. The measured V_{oc} was most likely a mixed potential or one with the H_2/H_2O ratio reflecting the amount (or rate) of methane being cracked [17]. SEM investigation showed that the anode consisted of submicron particles, which were essentially Ni particles since the anode comprised 42.5 vol.% Ni, 5.8 vol.% SDC, and 51.7 vol.% pores as shown in Table 1. Therefore, the anode had a large amount of surface area exposed to the methane. It is well known that nickel is a good catalyst for cracking C–H and C–C bond and has been used to catalyze the formation of carbon nanofibers [18,19]. Under these conditions, methane could be accelerated to crack via the pyrolysis reaction:

$$CH_4 = C + 2H_2 \quad (2)$$

Therefore, the lower V_{oc} observed with cell I is possibly due to methane cracking on the surface of nickel. Similar effects of fuel equilibriums at anode side on V_{oc}s were also observed for hydrocarbons by Gorte and co-workers [20,21]. V_{oc} for cells with impregnated SDCs are higher than that for cell I, ranging from 0.890 V for cell II to 0.902 V for cell IV. Although the V_{oc}s are still lower than the theoretical potential, the increase in V_{oc} seems to be an indication of the enhancement in direct electrochemical oxidation of CH_4 as shown in Eq. (1). In addition, the increase in V_{oc} may imply the suppression of the methane pyrolysis reaction.

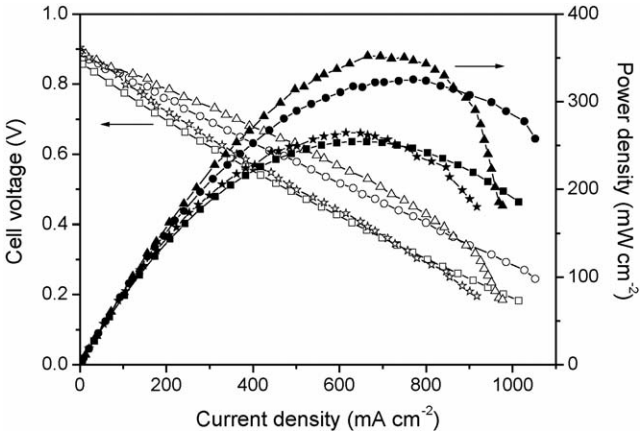

Fig. 4. Cell potentials (open symbols) and power densities (solid symbols) as a function of current density with humidified CH_4 as fuel at 600 °C for cell I (square), cell II (circle), cell III (triangle) and cell IV (star).

The cells, impregnated with nanosized SDC in the anode, also exhibited enhanced performance when methane was used as fuel. Shown in Fig. 4 is the cell performance when CH_4 was used as fuel. The performance increased with the amount of SDC impregnated in the anode up to its maximum of 20 mg cm^{-2}. With 20 mg cm^{-2} SDC in the anode, cell III achieved a maximum power density of 353 mW cm^{-2} at 600 °C with methane as fuel. The observed performance enhancement with methane as fuel was consistent with that when H_2 was used as fuel. Shown in Fig. 5 are the impedance spectra measured under open circuit conditions when humidified methane was used as fuel. The anode ASR was 0.308 Ω cm^2 for cell I in which there was no impregnation of SDC in the anode. It decreased with SDC impregnation in the anode to 0.181 Ω cm^2 for cell III. However, the ASR increased to 0.319 Ω cm^2 for cell IV where SDC impregnation higher than 20 mg cm^{-2}. As discussed above, the cell performance improvement is due to the enhanced TPB caused by the impregnated SDC. It is also due to the high catalytic activity of ceria toward hydrocarbon oxidation.

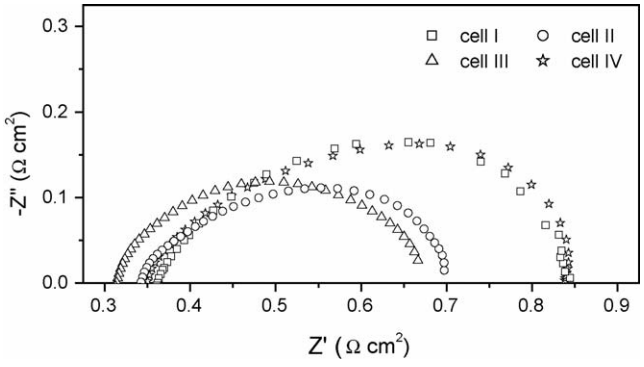

Fig. 5. Impedance spectra measured at open circuit condition for cells with humidified methane as fuels.

3.3. Stability of cells with CH_4 as fuel

The stability of cells operated with humidified methane as fuel was also characterized to assess the effect of carbon deposition on cell performance. Fig. 6 shows the stability of the different cells with a constant voltage load at 600 °C with humidified methane as fuel. Cell I decayed rapidly from 205 to 74 mW cm^{-2} within 7 h. After testing, carbon deposits could be seen on the anode surface. This serious carbon formation was predictable because of the high catalytic activity of nickel towards methane cracking. In contrast, stable operation over a 50 h period was observed for cells III and IV. In contrast to the severe degradation in cell performance for cell I, the outputs after 50 h operating were even higher than those achieved initially. No visible carbon was found on the anode surface of those two cells. Therefore, carbon deposition has been effectively suppressed in cells with SDC impregnated in the anode.

It is well known that carbon deposition is formed by a pyrolysis reaction such as Eq. (2) and the disproportionation of carbon monoxide such as:

$$2CO{=}C + CO_2 \quad (3)$$

which is thermodynamically preferred at temperatures above 700 °C. At temperatures below 650 °C, carbon deposition is mainly formed via the pyrolysis reaction. But the reaction rate is very slow without a catalyst such as Ni. For a cermet anode prepared with conventional ceramic processing techniques, such as anode for cell I and those reported previously [15], nickel usually has a volume fraction higher than 30 vol.% to meet the percolation limit. And the volume fraction of nickel and oxygen ion conductor phase such as SDC is often pretty close. Therefore, about half of the anode surface area is occupied by nickel. For example, about 88% surface is nickel for cell I and 60% for the cell previously reported [15]. The surface-seated nickel is believed to a good catalyst for fuel oxidation at the anode. However, when CH_4 is used as fuel, nickel is also a good catalyst for carbon deposition, which should be avoided in SOFC operation. Although pre-reforming is an effective way to overcome this problem, in-situ reforming and direct electrochemical oxidation at the anode is always a hot topic in SOFC research [3,22]. One possible way to avoid carbon deposition is to cover Ni particle with materials inert to carbon formation. Here we have demonstrated, for the first time that the cell stability has improved significantly when methane is used as fuel by covering nickel with nanosized SDC using the impregnation method. No carbon deposition was observed after operation of the cell with methane as fuel for 50 h. In addition to its function to prevent carbon deposition, the nanosized SDC is believed to be catalytic active for CH_4 oxidation. Finally, and possibly the most important, the coated SDC also serves as an oxygen ion conducting path to enlarge the TPBs and hence increase the cell performance as discussed above. It should be noted that it is possible that the nickel particle is not fully covered and unreachable by CH_4. Therefore, carbon deposition at the nickel surface is possible. However, the available nickel surface area is minimized, so that carbon formation would occur at a low level. The small amount of carbon can be removed with oxidation at the anode [23] and/or with H_2O which is formed at the anode.

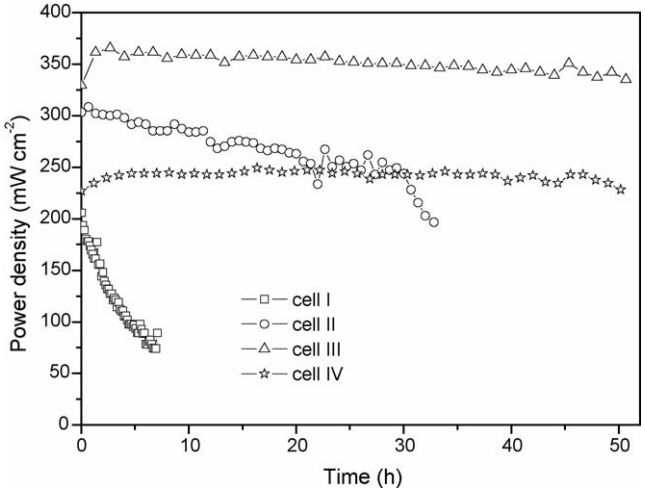

Fig. 6. Time dependence of power densities for cells operated at 600 °C with a constant output voltage of 0.5 V.

4. Conclusion

We have demonstrated that an anode-supported SOFC with a modified nickel-cermet anode running directly for methane exhibits good cell performance and long-term stability without carbon deposition. Nanosized SDC particles were coated uniformly onto the nickel particles of the anode using an ion impregnation method. When both humidified hydrogen and methane were used as fuel, the anode ASR decreased and cell performance increased with the SDC loading on the anode through this impregnation, inferring that the SDC coating on the nickel surface could effectively increase the number of triple-phase boundaries. The cells with 20 and 25 mg cm^{-2} SDC impregnated in the anode were operated at 600 °C for 50 h without obvious degradation when methane was directly used as fuel. This indicates that carbon deposition has been effectively suppressed. The advantage of this type of anode, i.e. a Ni framework coated with nanosized doped ceria, is that it shows high electrochemical activity towards hydrocarbon oxidation while inhibiting carbon formation from catalytic pyrolysis.

Acknowledgements

This work was supported by the Natural Science Foundation of China (50332040 and 50372066) and also by the China Ministry of Education (SRFDP20050358023).

References

[1] S. McIntosh, R.J. Gorte, Chem. Rev. 104 (2004) 4845–4865.
[2] E.P. Murray, T. Tsai, S.A. Barnett, Nature 400 (1999) 649–651.
[3] S.D. Park, J.M. Vohs, R.J. Gorte, Nature 404 (2000) 265–267.
[4] R.J. Gorte, S. Park, J.M. Vohs, C.H. Wang, Adv. Mater. 12 (2000) 1465–1469.
[5] S.W. Tao, J.T.S. Irvine, Nat. Mater. 2 (2003) 320–323.

[6] B.C.H. Steele, P.H. Middleton, R.A. Rudkin, Solid State Ionics 40–41 (1990) 388–393.
[7] O.A. Marina, C. Bagger, S. Primdahl, M. Mogensen, Solid State Ionics 123 (1999) 199–208.
[8] S.P. Jiang, S. Zhang, Y. Da Zhen, W. Wang, J. Am. Ceram. Soc. 88 (2005) 1779–1785.
[9] S.P. Jiang, S. Zhang, Y.D. Zhen, A.P. Koh, Electrochem. Solid State Lett. 7 (2004) A282–A285.
[10] C.R. Xia, W. Rauch, F.L. Chen, M.L. Liu, Solid State Ionics 149 (2002) 11–19.
[11] C.R. Xia, M.L. Liu, Solid State Ionics 144 (2001) 249–255.
[12] C.R. Xia, M.L. Liu, J. Am. Ceram. Soc. 84 (2001) 1903–1905.
[13] K. Eguchi, T. Setoguchi, T. Inoue, H. Arai, Solid State Ionics 52 (1992) 165–172.
[14] M. Godickemeier, L.J. Gauckler, J. Electrochem. Soc. 145 (1998) 414–421.
[15] Y.H. Yin, W. Zhu, C.R. Xia, C. Gao, G.Y. Meng, J. Appl. Electrochem. 34 (2004) 1287–1291.
[16] S. McIntosh, J.M. Vohs, R.J. Gorte, J. Electrochem. Soc. 150 (2003) A1305–A1312.
[17] M. Mogensen, K. Kammer, Ann. Rev. Mater. Res. 33 (2003) 321–331.
[18] P. Chen, H.B. Zhang, G.D. Lin, Q. Hong, K.R. Tsai, Carbon 35 (1997) 1495–1501.
[19] M.L. Toebes, J.H. Bitter, A.J. van Dillen, K.P. de Jong, Catal. Today 76 (2002) 33–42.
[20] S. McIntosh, J.M. Vohs, R.J. Gorte, Electrochem. Solid State Lett. 6 (2003) A240–A243.
[21] S. Park, R. Craciun, J.M. Vohs, R.J. Gorte, J. Electrochem. Soc. 146 (1999) 3603–3605.
[22] B. Morel, J. Laurencin, Y. Bultel, F. Lefebvre-Joud, J. Electrochem. Soc. 152 (2005) A1382–A1389.
[23] J. Liu, S.A. Barnett, Solid State Ionics 158 (2003) 11–16.